Title: Design and evaluation of additively manufactured parts with three dimensional continuous fibre reinforcement.

Abstract:

Additive manufacturing (AM) provides many benefits such as reduced manufacturing lead times, streamlined supply chains, part consolidation, structural optimisation and improved buy-to-fly ratios. Barriers to adoption include high material and processing costs, low build rates, isotropic material properties, and variable processing conditions. Currently AM polymer parts are far less expensive to manufacture than AM metal parts, therefore improving the properties of polymer parts is highly desirable.

This paper introduces a design methodology used to integrate continuous reinforcement into AM polymer parts with the aim of improving their mechanical properties. The method is validated with the design and testing of three case studies, a pulley housing, hook and universal joint used to demonstrate the applicability of the method for tensile, bending and torsion loading types respectively.

Physical testing showed that it was possible to improve the strength of parts by over 4000%, elongation to failure by over 2000% and stiffness by approximately 200%. In addition a method of integrating condition monitoring capabilities into the parts was demonstrated.
An analysis of the specific strength of the parts suggests that the reinforced parts are comparable to aluminium alloys, suggesting that in some cases AM polymer composite parts could supplant more costly metal parts.

Graphical abstract:
Evolution of a pulley design from left to right: a) volumetric design space, b) topological optimisation, c) FEA of fibre reinforced part, d) final iteration after first physical tests.

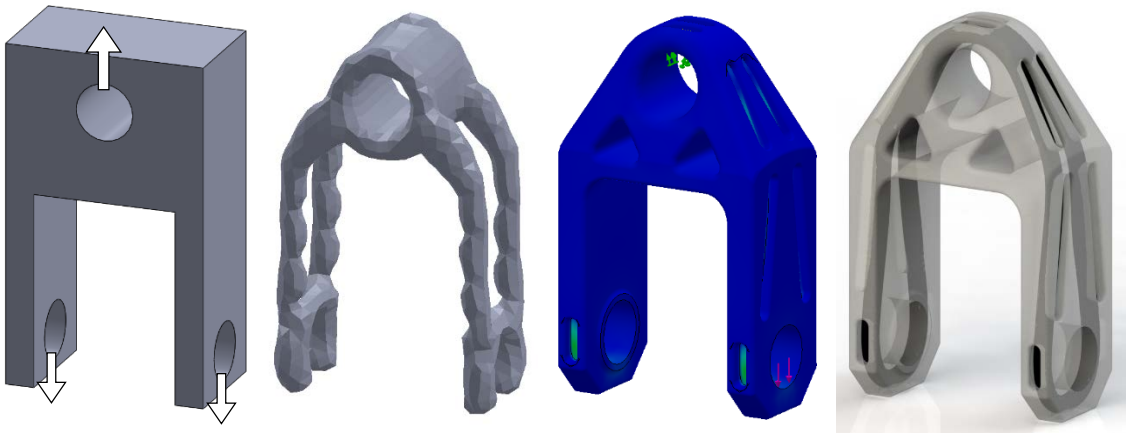

a) b) c) d)

Highlights:

- New design methodology for AM parts with continuous reinforcement
- Verified methodology with three case studies
- Improved strength by over 4000% and elongation to failure by over 2000%
- Introduced method of integrating sensors

Keywords
Carbon fibre, Polymer-matrix composites, Mechanical properties, Finite element analysis, Additive manufacturing, Condition monitoring.

1. Introduction

Additive manufacturing (AM) is seeing increased utilisation in sectors such as aerospace and motorsports due to its ability to produce parts with high geometrical complexity and short manufacturing lead times [1]. Revenues from the production of end use parts, as a proportion of total AM production, has risen from under 4% in 2003 to 34.7% in 2013 [2]. Both Airbus and Boeing are currently producing aircraft with AM polymer parts while GE Aviation incorporates AM metal parts in its commercial jet engines [3]. These AM parts offer many advantages such as optimised geometries for structural loads, better flow characteristics and part consolidation. AM also helps to streamline manufacturing enabling highly responsive manufacture of short-run orders and replacement parts [4]. To date AM as a proportion of the total manufacturing sector is still very low due to the high cost of AM machines and materials, variable processing conditions, material quality issues and low volumetric deposition rates [5]. These drawbacks are

currently restricting the use of high specific strength alloys such as Al-Si-10Mg and Ti-6Al-4V produced via AM [6]. Conversely, additively manufactured polymer parts have relatively favourable economics but suffer from inferior mechanical and thermal properties [7, 8].

One of the main drivers for the adoption of AM is the lightweighting of parts and assemblies. By optimising design for function and reducing the buy-to-fly ratio it is possible to significantly reduce life cycle energy use and materials costs [9, 10]. For similar reasons metals are being replaced with polymers and polymer matrix composites (PMCs). PMCs are already routinely used in aerospace and motorsport to replace metal parts due to excellent strength to weight ratios and fatigue properties [11]. Unfortunately PMCs with continuous fibres require a range of processing methods and tools that limit the design freedoms and turnaround times when compared with AM. The exception to this is extrusion based AM machines which embed reinforcement in layers along with the polymer beads e.g. the Mark One manufactured by Markforged. Currently this method only allows fibre to be laid in the horizontal plane. Short fibre reinforced polymers may be processed by conventional AM technologies such as Fused Filament Fabrication (FFF) and Selective Laser Sintering (SLS) however these only provide modest increases in material strength [12].

This work outlines how hybrid AM parts can be reinforced to create complex, low weight, low cost, high strength parts. As AM polymers accounted for 98% of the AM materials market in 2013 any improvements to the properties of AM polymer parts could have a large commercial impact [13].

The following section will describe the design methodology used to determine the location of the fibre reinforcement, followed by the results of finite element analysis and physical testing.

2. Design methodology

The aim of this methodology is to design channels within the parts that may be filled with continuous reinforcement and will take the majority of the load. The first condition for applying this methodology is that the loads are well specified. The specific placement of the reinforcement will greatly improve the strength of the parts for the known loads, however the part will retain the polymer material strength in other directions. Assuming this condition is met then the iterative design process can be summarised according to figure 1.

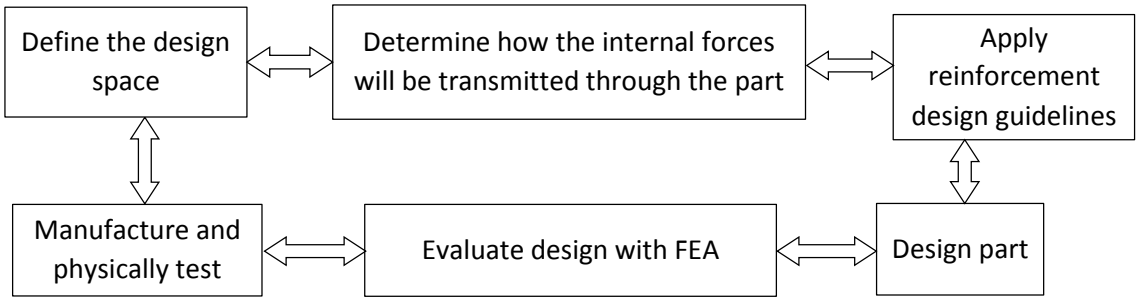

Figure 1. Schematic of the design process.

In the following sections a simple pulley housing will be used to demonstrate the design methodology.

2.1 Define the design space

The first step is to define the volume the part may occupy and how the loads are going to be applied. The volumetric design space should be represented as simply as possible and guided only by bounding dimensions as shown in Figure 2.

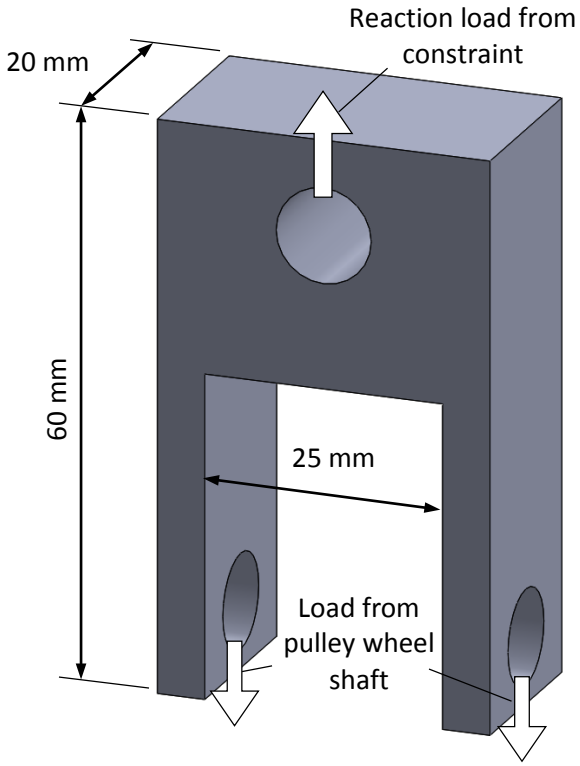

Figure 2. 3D representation of the volumetric design space

2.2 Determine internal load paths

The second step is to determine where within the volumetric design space load carrying material is needed. In this process the load carrying material is assumed to be the

reinforcement, whilst the polymer is considered a preform that holds the reinforcement in place. Assuming the reinforcement is much stiffer than the polymer material (*Er* >> *Em*) it will take a proportionately higher percentage of the load, as demonstrated by applying the rule of mixtures to the Voigt model for axial loading [14].

$$E_c = \sigma_c/\varepsilon_c = \frac{(1-f)\sigma_m + f\sigma_r}{(\sigma_r/E_r)} = (1-f)E_m + fE_r \qquad \text{Equation (1)}$$

The force lines method is a powerful qualitative way of visualising how the internal load travels through the part, and is a good analogy for how reinforcement carries the load in PMCs [15]. For complex loading states a quantitative method, such as topological optimisation, may be needed. It should be apparent that for the case of the pulley housing both results point towards similar geometries (figure 3). The granularity of the topological optimisation in figure 3 is primarily due to the resolution of the initial FEA and the step size of the volume fraction reductions. The boundary conditions also have a large impact on the optimised shape, as evidenced by the top hole which was set as a fixed face and the bottom holes which were not.

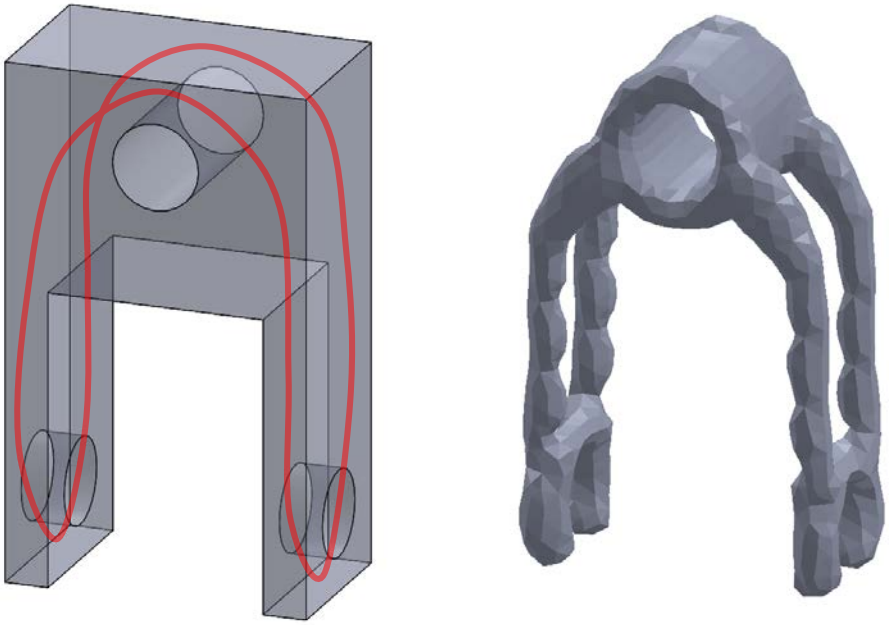

Figure 3. Qualitative force lines method (left). Quantitative topological optimisation (right).

2.3 Apply the reinforcement design guidelines

The geometries shown in figure 3 are only to be used as a guide as to where the reinforcement should be placed. Due to the fact the topological optimisation assumed isotropic material properties it is not a perfect analogy for fibre placement. Reinforcement design guidelines

inspired by tensegrity should additionally be used to find path geometries that minimise the load in the polymer [16]. These guidelines are as follows:

1. The reinforcement path should go through all areas of high Von Mises stress but be aligned with the first or second principal stresses.
2. The reinforcement path should be continuous with as few discreet loops as possible.
3. In areas of high tensile load the fibre centre of curvature should be directed into the part and not away from the surface. This reduces the likelihood of the fibre separating from the part.
4. Internal channels as an alternative to open channels can help to improve bonding between the reinforcement and the part and also delays fibre buckling in compressive areas.
5. The beginning and end points of the reinforcement should be in areas of low stress.
6. Access ports are needed to allow the reinforcement to be fed into any internal channels. The number and length of access points will depend on the part geometry and the form of the reinforcement.
7. Points of inflexion may need to be accessible as they can complicate winding.

The last three points are primarily design for manufacture guidelines. Figure 4 shows the final design of the pulley housing with a few modifications for aesthetics, weight reduction and design for AM considerations.

Figure 4. Pulley housing with reinforcement channel and access ports.

In the example of the pulley housing above it is relatively straight forward to meet the reinforcement design guidelines, however, if the upper hole was rotated 90° about the vertical axis, two discreet channels (or a crossover point) will have been necessary. This demonstrates why the process needs to be iterative and how the reinforcement guidelines may require the loads or constraints to be applied in a different orientation than originally intended.

In practice it may also be necessary to add metal threaded inserts or compression limiters to critical holes or features. This is relatively easy to do by heat staking the insert into the receiving hole. No inserts were used in this work so that the effect of the reinforcement alone may be demonstrated.

2.4 Mechanical Analysis

The next stage is to simulate part loading to assess whether any design iterations are necessary. For the pulley housing a static finite element analysis was used to visualise the stress distributions. The reinforcement material properties were modelled as unidirectional continuous carbon fibre in an epoxy matrix with a volume fraction of 60%, whilst the polymer was Polyamide 12. The materials are anisotropic, however for simplicity the materials were assumed to be isotropic. Due to the fact the reinforcement is not supporting high shear loads, and the polymer is carrying a very low proportion of the load, the simulation is deemed accurate enough to evaluate the altered stress distributions. Perfect bonding was assumed between the reinforcement and the polymers. Figure 5 shows the stress distribution for a non-reinforced and reinforced pulley with a load of 500N. The non-reinforced part clearly experiences a higher level of stress throughout the polymer volume. The isoclip of the reinforced part shows how all the stress over 15MPa is held within the reinforcement while the polymer experiences negligible stress.

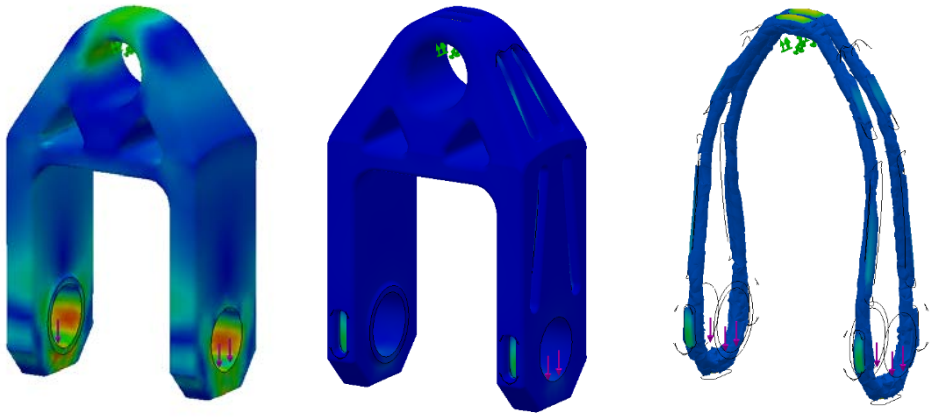

Figure 5. Results of static finite element stress analysis for an un-reinforced part (left), reinforced (middle) and an isoclip of the reinforced part showing areas over 15MPa only (right).

The pulley housing represents a part with predominantly tensile loading. Figures 6 and 7 show two further parts; a hook and a universal joint (half), designed to demonstrate the applicability of the methodology to real world bending and torsion applications respectively.

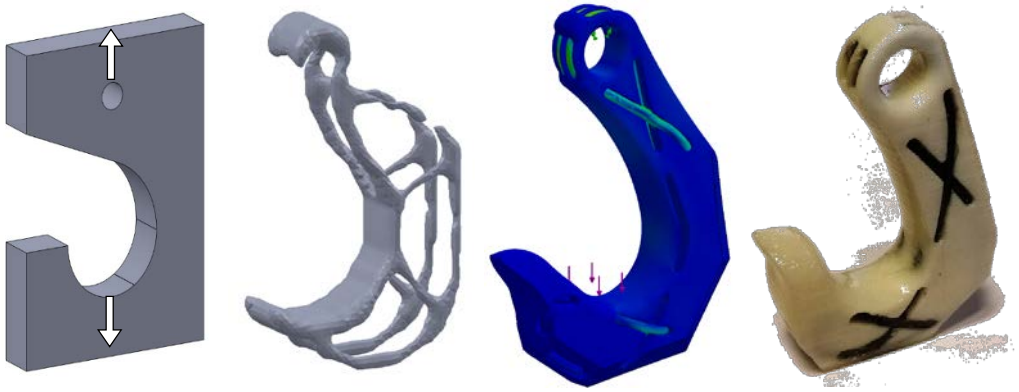

Figure 6. Evolution of the hook design from left to right: volumetric design space, topological optimisation, FEA of composite, final iteration after first physical tests.

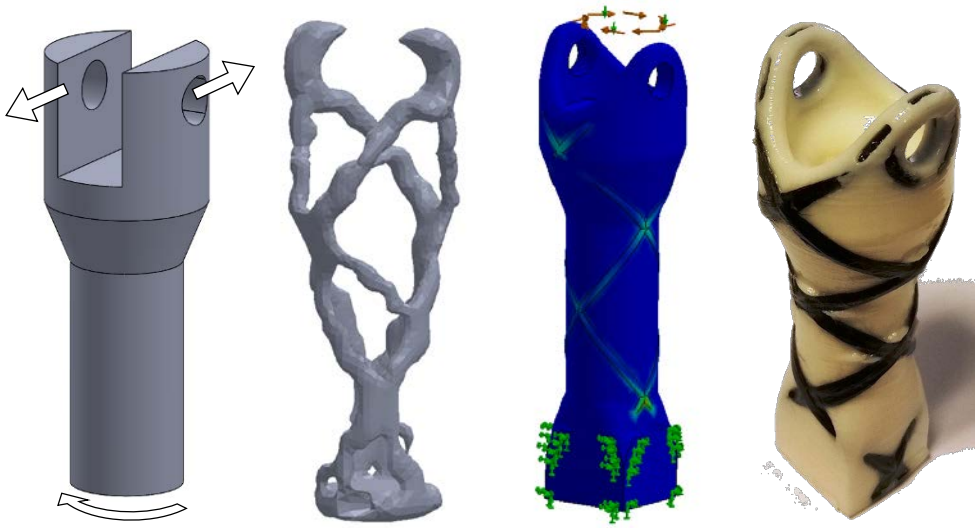

Figure 7. Evolution of the universal joint design from left to right: volumetric design space, topological optimisation, FEA of composite, final iteration after first physical tests.

The results of physical testing of all three designs are presented in the following section.

3. Manufacture and Physical testing

A range of polymer and reinforcement material combinations were tested. Fused filament fabrication (FFF) was used to print polylactic acid (PLA) and acrylonitrile butadiene styrene (ABS). The PLA parts were printed on a MakerGear M2 with FormFutura filament whilst the ABS parts were printed on a da Vinci 1.0A with da Vinci ABS filament. Selective laser sintering (SLS) was used to print Polyamide 12 (PA12) parts. The parts made by FFF consisted of 0.2 mm layers with 25-50% infill and were printed with the layers perpendicular to the direction of the principal stress i.e. the least favourable orientation for strength. The PA12 part was printed with the layers parallel to the principal stresses i.e. the most favourable orientation for strength.

Carbon, Kevlar, basalt and 316 stainless steel wire cord (Ø 1.5 mm) were all used for reinforcement. All reinforcement channels were modelled with 2.8 mm nominal diameters, however due to the variations in manufacturing processes (particularly with FFF) the channel diameters ranged from 2.3 mm to 2.8 mm.

Carbon, Kevlar and Basalt fibres were sourced in tow form (untwisted bundles of unidirectional fibres). The tows were then cut to length and cyanoacrylate glue was used to create nibs on each end. Each tow was then threaded through the part in a similar fashion to lacing shoes. Once the channels were filled any excess fibre was cut off and the threaded fibres were held in place with a small amount of cyanoacrylate glue in a low stress area. A low viscosity epoxy

laminating resin, EL2 from Easy Composites™, was used to bond the reinforcement within the channels. Threaded parts were submerged in the resin and a brush was used to encourage complete infiltration of the reinforcement channels. Excess resin was then allowed to drain from the part before being cured in an oven at approximately 50°C overnight. Copper ferrules were used to fix the loose ends of the stainless steel cord instead of epoxy. This required a slight modification of the design to allow space for the ferrule. Total lead time for the construction of one pulley was approximately 24 hours. This included 40 minutes printing time and 30 minutes of labour to thread and epoxy each pulley. The majority of the time was spent curing the epoxy.

The pulley housings and hooks were tested on a Testometric FS100SCCT 100KN universal testing machine with a constant strain rate of 2.5 mm/min. Figure 8 shows the experimental apparatus. In all cases un-reinforced parts (with the channels removed) were tested for reference.

Figure 8. Fixtures for pulley and hook tests.

The universal joint design was tested on a manual torsion rig and torqued in 2.49 Nm increments (figure 9). After each weight was added to the lever arm a torque was applied to the end of the part until the weighted lever arm returned to horizontal. The change in angle was then measured and the process repeated.

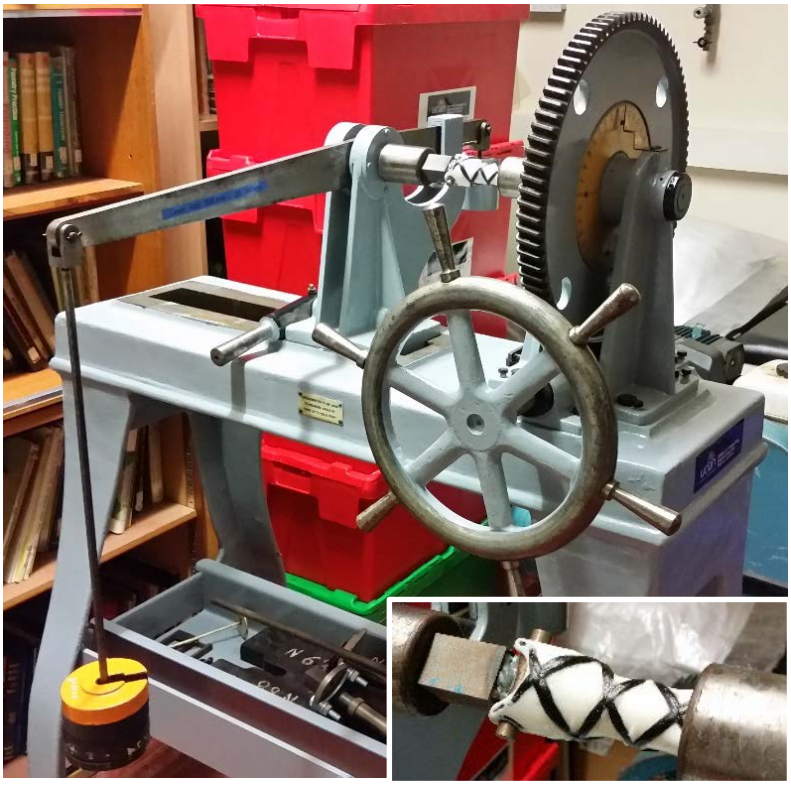

Figure 9. Manual torsion testing machine. Bottom right insert: close up of universal joint half with fixtures and constraints.

4. Results

In all cases the reinforced parts showed significant increases in part strength, toughness, elongation to failure and stiffness over the unreinforced parts. A summary of the results for the various pulley material combinations is shown in Table 1.

Table 1. Maximum load and elongation at maximum load for a variety of polymer/reinforcement pulley combinations.

Reinforcement	3D printed pulley					
	PLA		ABS		PA12	
	Load (N)	Elongation (mm)	Load (N)	Elongation (mm)	Load (N)	Elongation (mm)
None	928	1.07	152	0.34	1503	1.62
Carbon	8002	6.65	7280	7.86	8816	7.74
Kevlar	-	-	7645	9.39	-	-
Stainless steel	-	-	2906	5.78	-	-
Basalt	3647	3.41	-	-	-	-

The strongest combination was found to be PA12 with carbon fibre reinforcement. PLA and carbon fibre was a close second suffering from a more anisotropic structure and a sparse infill.

In most cases the stiffness of the parts increased approximately 200%, whilst the elongation to failure, in the case of ABS and Kevlar, increased by 2660%. Failure typically occurred in the polymer whilst the reinforcement remained intact and still able to support significant loads. The stainless steel reinforcement was found to fail prematurely due to imperfect crimping of the ferrules.

Figure 10 shows the load-displacement curves for PLA pulley housings with and without carbon fibre reinforcement. The unreinforced pulley failed in the lower leg near the hole as predicted by the FEA. The reinforced part exhibited steady deformation around the holes with minor cracks forming in the polymer/resin at around 2 mm of elongation (3.3% strain). Final failure of the reinforcement occurred near the holes, again in agreement with FEA predictions.

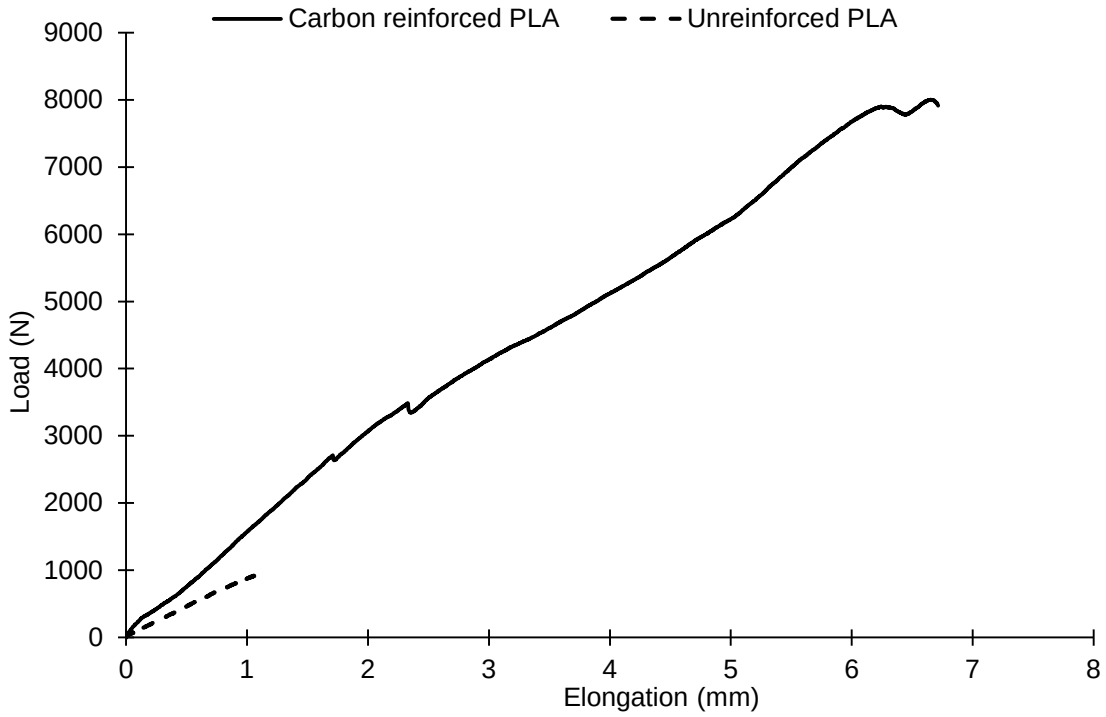

Figure 10. Load-elongation curves for PLA pulley housings with and without carbon reinforcement.

The reinforced PLA pulley exhibited a 762% increase in strength over the unreinforced PLA pulley and a 521% increase in the elongation to failure.

The hook and universal joints also showed significant gains in strength and toughness as shown in figure 11. The universal joint showed the smallest gain in improvement. Coincidently it was the only part designed with the fibre wrapped on the outside of the part. This was done to maximise the parts polar moment of inertia but also allowed the fibres, which were in

compression, to buckle and delaminate from the parts surface. This observed failure mode may go some way towards explaining the performance of the universal joint test pieces.

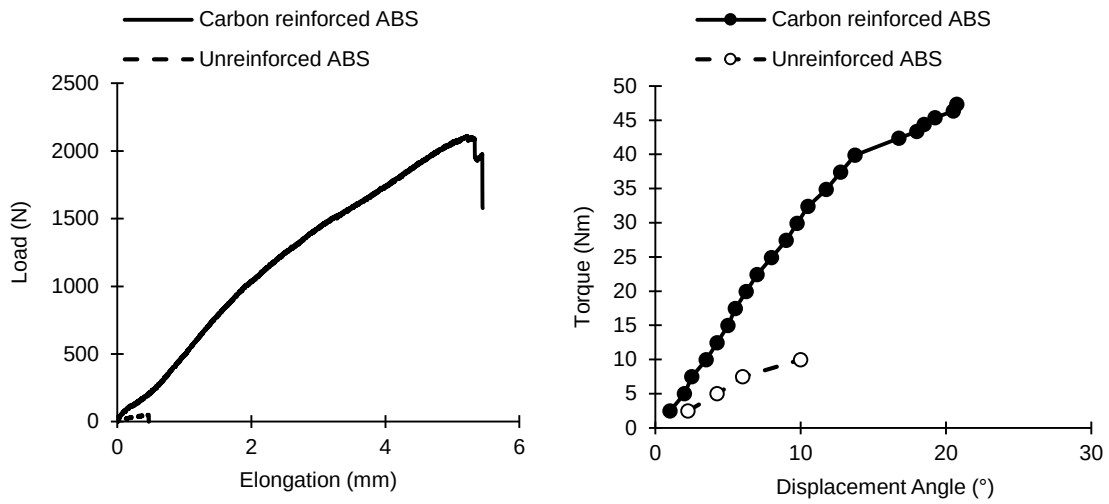

Figure 11. Load-elongation curves for ABS hooks with and without carbon reinforcement (left). Torque-rotation curves for ABS universal joints with and without carbon reinforcement (right).

Despite the three parts having markedly different geometries and loading conditions the load-displacement curves are all fairly similar. A possible reason for this is the fact that the reinforcement fibres are predominantly orientated in the direction of the 1st and 2nd principal stresses and therefore all react in a similar way. The shape of the curves is similar to that you would expect for a polymer, only scaled up. The pulley housings demonstrated the largest improvement in mechanical properties due to the fact the reinforcement only supported tensile stresses, unlike the other parts which also had compressive stresses.

Figure 12 compares the performance of the pulley housings, hooks and universal joints in unreinforced ABS, reinforced ABS and reinforced PLA.

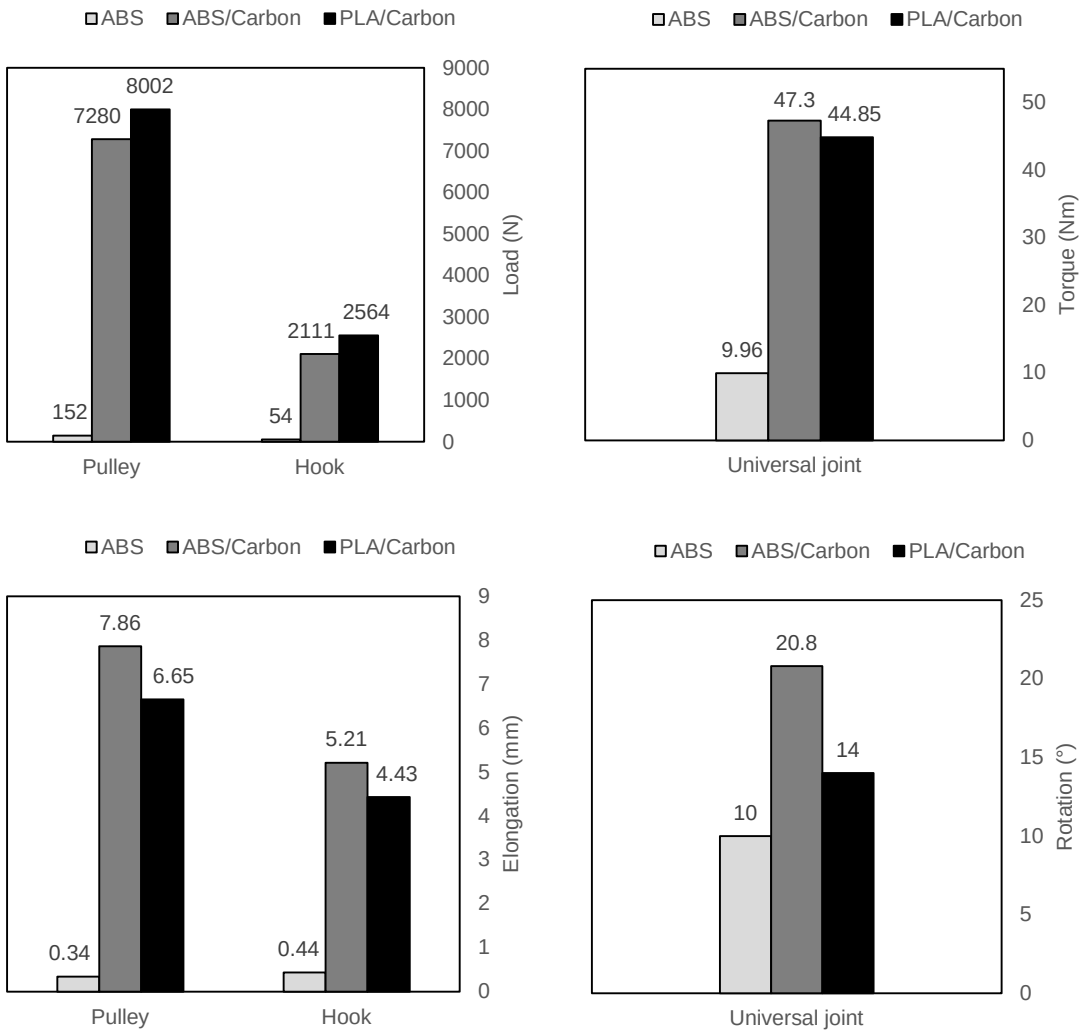

Figure 12. Left: Load-elongation data for pulleys and hooks. Right: Torque-rotation data for the universal joints.

All pulley parts were printed with 25% infills. Comparing the reinforced ABS with the reinforced PLA shows that there is a slight trade-off between strength and elongation to failure between the two polymers. This is expected as PLA is stronger and less ductile than ABS. The ABS hooks and universal joints were printed with a 50% infill density compared with 25% for the PLA. This is the likely reason for why the ABS outperformed the PLA in the case of the universal joint. Why the difference in infill significantly affected the universal joint performance but not the hook is not fully understood and needs further investigation.

4.1 Inbuilt sensing

Due to the unique location of the reinforcement channels they may be used to add extra functionally to the parts, such as condition monitoring capabilities. As a proof of concept, Kanthal resistance wire Ø 0.15 mm (28 Ω/m) was added to the carbon fibre reinforcement of a pulley housing. 100 mm of wire was left protruding from the entry and exit points so that a multi-

meter could measure the resistance across the wire. The pulley was tested in the universal testing machine at a strain rate of 1 mm/min whilst the load, elongation and resistance where recorded at 5 second intervals.

Figure 13 shows the change in resistance with elongation for the test. Unfortunately the multi-meter only measured to 0.1 Ω so the captured data contains significant uncertainty. Plotting a line of best fit (least squares method) shows a fairly strong linear correlation with an R^2 value of 0.797. Using smaller diameter wires or increasing the length of embedded wire will help to amplify the signal. This sensing capability could be used for structural health monitoring or fatigue analysis and would be particularly useful for large scale parts and assemblies.

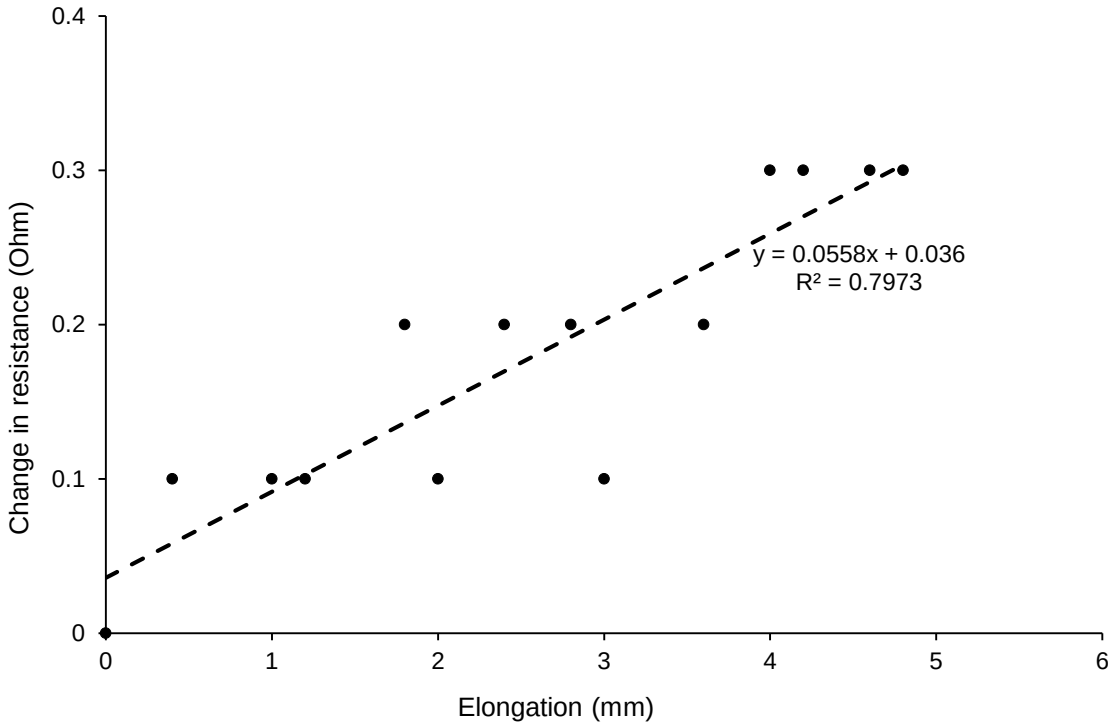

Figure 13. Change in resistance with elongation for embedded resistance wire in a pulley housing.

Replacing the reinforcement fibre with piezoelectric fibres may provide an ideal way to incorporate high frequency low amplitude actuation into parts with complex geometries.

5. Discussion

The methodology outlined in this paper allows significant improvements to the capabilities of polymer AM parts with minimal quantities of reinforcement. On the downside extra design and manufacturing time increases the part costs over unreinforced parts. To determine if the benefits outweigh the drawbacks it is useful to compare the performance of the composite parts

with other relevant materials. From the load, cross-sectional area and stress concentration at the point of failure, it is possible to calculate an effective tensile strength (σ_{eff}) for the composite pulleys (Equation 2 and 3) [17, 18].

$$\sigma_{eff} = K\sigma_{nom} = K\,F_{max}/A_F \quad \text{Equation (2)}$$

$$K = 3.00 - 3.14\,D/W + 3.67(D/W)^2 - 1.53(D/W)^3 \quad \text{Equation (3)}$$

Where K = Stress concentration for a hole in a plate, F_{max} = the load acting on A_F, A_F = the cross-sectional area at the failure point, D = hole diameter, W = width of material at the point of failure. The effective tensile strength for PA12 and PA12/PLA parts reinforced with carbon fibre are shown in table 2.

Understandably, the effective tensile strength calculated using this method is not a true material property but a function of loading, geometry and the volumetric ratio between reinforcement and polymer. In the case of the pulley leg the reinforcement channel almost completely filled the internal part volume around the hole, providing a natural limit to the amount of reinforcement able to be applied. Increasing the design space would allow for more reinforcement however it should not be assumed that the part strength will simply increase in proportion to the added reinforcement. A limit exists whereby failure moves to an unreinforced part of the polymer. Once this limit is reached then increasing the size of the existing channels has little effect and new reinforcement channels are required.

For high performance industries such as transport and sport, the strength to weight ratio is often more important than the absolute material strength. Table 2 compares how the composite AM parts compare with other common engineering materials, if used in a similar context. The reinforced AM parts were weighed, whilst the pulley weights of the other materials were calculated in Solidworks. Unless otherwise stated all material property data was sourced from the Solidworks materials database.

Table 2. Comparison of different potential pulley materials density and strength.

Pulley material	Pulley weight (g)	Density (kg/m³)	Tensile strength (MPa)	Specific strength (kPa/(kg/m³))
PA12	13.3	950	32**	34
PA12 + Carbon	14.0*	1066	190**	178
PLA + Carbon	12.8*	975	170**	174
Al-Si-10Mg	36.8	2680	337	123
7075 – T6	38.6	2810	570	203
Ti-6Al-4V	60.9	4429	1050	237
316 SS	110.0	8000	550	69

*Weighed before testing. **Effective tensile strength calculated by equations 1 and 2.

The specific strength of the reinforced polymer pulleys is comparable to that of Al-Si-10Mg and 7075 – T6, aluminium alloys used in the aerospace industry, and are over double the specific strength of 316 stainless steel. The material costs and manufacturing times for metal AM parts are currently an order of magnitude higher than for polymers [6-8, 19]. These results suggest that utilising polymers with minimal additions of reinforcement can create high strength parts at a fraction of the cost and manufacturing time required for metal AM parts. Using natural fibres such as flax or basalt in combination with PLA also provides options with lower environmental impact [20].

The parts tested in this paper were of the order of 125 cm^3 however it is believed that the method could be successfully scaled for larger parts. Replacing loose fibre tows with cord or rope is an effective way to reduce threading time. How the reinforcement distributes the loads to the polymer at large scales will need to be carefully considered to avoid concentrated forces. Elliptical or 'flat' channels can be used to help distribute the internal loads. The use of metallic inserts and compression limiters will likely be essential in most cases.

Accurate simulation of these parts is difficult due to the composite nature of the materials, the organic geometries and complex stress states. Therefore integrating sensing technology into the parts may prove extremely useful.

6. Conclusions and recommendations

This paper introduced a new methodology for designing AM polymer composite parts. The methodology was validated by designing and testing three parts with tensile, bending and torsion loads respectively. A wide range of polymer/reinforcement combinations were tested including low environmental impact materials.

The reinforced parts showed significant improvements in strength, stiffness and toughness over non-reinforced parts. An analysis of the specific strength of the pulley housing showed the reinforced polymers to be comparable with common aerospace aluminium alloys. The method is believed to be scalable and can produce parts with short manufacturing lead times.

Further research is needed to determine if the methodology may be used to reinforce 3D printed metals, ceramics and polymers for high temperature applications.

In line with the novelty of the introduced method there are still many opportunities for future developments. The time taken to design the parts could be significantly reduced by developing a quantitative force line analysis tool that uses FEA results as input data. This has already been shown to be possible for 2D problems [15]. Extending a quantitative force lines tool to three dimensional assemblies would also be of immense benefit to design engineers.

Manual threading of the fibres is very labour intensive, requires access holes, and is a major source of performance variability. Innovative methods of introducing the fibres, such as using air jets or magnets to lead the fibres through the channels would drastically reduce labour and process variability.

There is a need for in-depth analysis of the failure modes under different loading conditions. Fibre pull out, fibre delamination, fibre buckling, tensile yielding, sparse infill crushing and delamination of the printed layers are all failure modes that have been witnessed but cannot currently be predicted.

A full cost comparison is needed to compare the economic and environmental costs of reinforced 3D printed parts with conventional manufacturing methods. This is crucial information for decision makers within companies who will need to weigh the risks of adopting this methodology against the potential benefits.

Whilst the strength, toughness and elongation to failure have all been dramatically improved with this method there are a number of extremely important surface properties such as hardness, friction and wear that are left unchanged. Research is ongoing to test whether coatings can be used to significantly improve surface properties. In addition novel internal structures and infills are being investigated for their ability to improve the parts thermal properties.

Finally the condition monitoring capabilities demonstrated in this work were not sensitive enough to be of practical use. Further research is needed to develop higher resolution inbuilt sensors and to investigate whether it is practical to create smart parts that can sense and respond to changing environments whilst communicating via the internet of things.

7. Acknowledgements

I would like to thank the University of Central Lancashire Centre for Research Informed Teaching (CRIT) for the Undergraduate Research Internship Scheme funding which aided the completion of this work.

8. References

1. Rawal, S., J. Brantley, and N. Karabudak. *Additive manufacturing of Ti-6Al-4V alloy components for spacecraft applications*. in *Recent Advances in Space Technologies (RAST), 2013 6th International Conference on*. 2013.

2. Wohlers, T., *Wohlers Report 2014: 3D Printing and Additive Manufacturing State of the Industry Annual Worldwide Progress Report*. 2014: Wohlers Associates.
3. Lyons, B., *Additive manufacturing in aerospace: examples and research outlook.* The Bridge, 2014. 44(3).
4. Khajavi, S.H., J. Partanen, and J. Holmström, *Additive manufacturing in the spare parts supply chain.* Computers in Industry, 2014. 65(1): p. 50-63.
5. Gibson, I., D. Rosen, and B. Stucker, *Additive Manufactruing Technologies*. 2010: Springer US.
6. Baumers, M., et al. *Combined Build-Time, Energy Consumption and Cost Estimation for Direct Metal Laser Sintering*. in *From Proceedings of Twenty Third Annual International Solid Freeform Fabrication Symposium—An Additive Manufacturing Conference*. 2012.
7. Ruffo, M., C. Tuck, and R. Hague, *Cost estimation for rapid manufacturing - laser sintering production for low to medium volumes.* Proceedings of the Institution of Mechanical Engineers, Part B: Journal of Engineering Manufacture, 2006. 220(9): p. 1417-1427.
8. Wittbrodt, B.T., et al., *Life-cycle economic analysis of distributed manufacturing with open-source 3-D printers.* Mechatronics, 2013. 23(6): p. 713-726.
9. Chu, C., G. Graf, and D.W. Rosen, *Design for additive manufacturing of cellular structures.* Computer-Aided Design and Applications, 2008. 5(5): p. 686-696.
10. Huang, R., et al., *Energy and emissions saving potential of additive manufacturing: the case of lightweight aircraft components.* Journal of Cleaner Production, 2015(0).
11. Jerome, P., *Composite materials in the airbus A380-from history to future.* 2001.
12. Yan, C., et al., *Characterisation of carbon fibre reinforced nylon-12 composites for selective laser sintering process*, in *Innovative Developments in Virtual and Physical Prototyping*. 2011, CRC Press. p. 355-358.
13. IDTechEx, *3D Printing Materials 2014-2025: Status, Opportunities, Market Forecasts*. 2013: Market Research Report.biz.
14. Mallick, P.K., *Composites engineering handbook*. 1997: CRC Press.
15. Kokcharov, I. and A. Burov, *Analysis of stress state with the force lines method.* choice, 2001. 10: p. 2.
16. Pugh, A., *An introduction to tensegrity*. 1976: Univ of California Press.
17. Budynas, R.G. and J.K. Nisbett, *Shigley's Mechanical Engineering Design*. 2008: McGraw-Hill.
18. Pilkey, W.D., *Formulas for Stress, Strain, and Structural Matrices*. 1994: Wiley.
19. Santos, E.C., et al., *Rapid manufacturing of metal components by laser forming.* International Journal of Machine Tools and Manufacture, 2006. 46(12–13): p. 1459-1468.
20. Gurunathan, T., S. Mohanty, and S.K. Nayak, *A review of the recent developments in biocomposites based on natural fibres and their application perspectives.* Composites Part A: Applied Science and Manufacturing, 2015. 77: p. 1-25.